JOURNAL OF MATERIALS SCIENCE 29 (1994) 4431–4435

The stress dependence of Barkhausen noise in $Fe_{81}B_{13.5}Si_{3.5}C_2$ Metglas

H. C. KIM, DONG YOUNG KIM
Physics Department, The Korea Advanced Institute of Science and Technology, 373-1 Kusong-Dong, Yusung-Gu, Taejon, 305-701, Korea

C. G. KIM
Magnetics Laboratory, Korea Research Institute of Standards and Science, Taedok Science Town, PO Box 3, Taejon, Korea

The Barkhausen noise (BN) profile of $Fe_{81}B_{13.5}Si_{3.5}C_2$ Metglas changes from single to double peaks with applied tensile stress. The second harmonics during the magnetization process under various stresses confirm that the single and double peaks on the BN profiles can be attributed to domain nucleation/annihilation. The variation of the initial permeability with tensile stress indicates that the volume fraction of longitudinal domains along the stress direction increased up to a stress of 20 MPa (stage I) and then it remained constant with further stressing, $v_{\parallel}(\sigma) \approx 1$ (stage II). The total BN activity during a half (B–H) loop with tensile stress, transient also at about 20 MPa, can be characterized by a $(BN)_{tot} \propto e^{\beta\sigma}$ relationship, where the exponents are $\beta_1 = 1.761 \times 10^{-2}$ and $\beta_2 = 1.758 \times 10^{-3}$ for stages I and II, respectively. An analysis of $(BN)_{tot}$ in stage II showed that the number of domains involved in the domain nucleation/annihilation is proportional to $\sigma^{1/2}$.

1. Introduction

A magnetization process represented by a hysteresis loop which is not continuous, consists of discrete jumps of the microscopical magnetization, (and these sudden changes of the irreversible magnetic flux) is referred to as magnetic Barkhausen noise (BN). The high Barkhausen activity at the field of maximum susceptibility in plastically deformed 3% SiFe [1] and $Fe_{40}Ni_{38}Mo_4B_8$ metallic glass [2] and at the knees of the hysteresis loop in annealed crystalline materials [3, 4] can be attributed, respectively, to the domain-wall motion and the domain nucleation/annihilation occurring during the magnetization process. Previous papers [5–7] showed that the BN increases or decreases with stress depending on whether tensile or compressive stresses, respectively, are applied. However, no comprehensive physical model is yet available which accounts for the stress dependence of the BN characteristics associated with the domain dynamics in amorphous and crystalline materials.

In this paper, the variations of the BN profile with the magnetic field and the integration of a BN profile during a half B–H loop, $(BN)_{tot}$, was studied in $Fe_{81}B_{13.5}Si_{3.5}C_2$(2605SC) Metglas under various applied tensile stresses. The results are discussed in terms of domain nucleation/annihilation and the volume fraction of longitudinal domains caused by magneto-elastic coupling with the applied tensile stress.

2. Experimental procedure

The measurements were performed on a commercially available 2605SC amorphous ribbon (supplied by Nippon Metallic Amorphous Ltd.), with dimensions of 2.5 cm × 11 cm × 25 μm, in the as-received state.

A block diagram of the BN measurements is shown in Fig. 1. Two coils for detecting BN were wound with

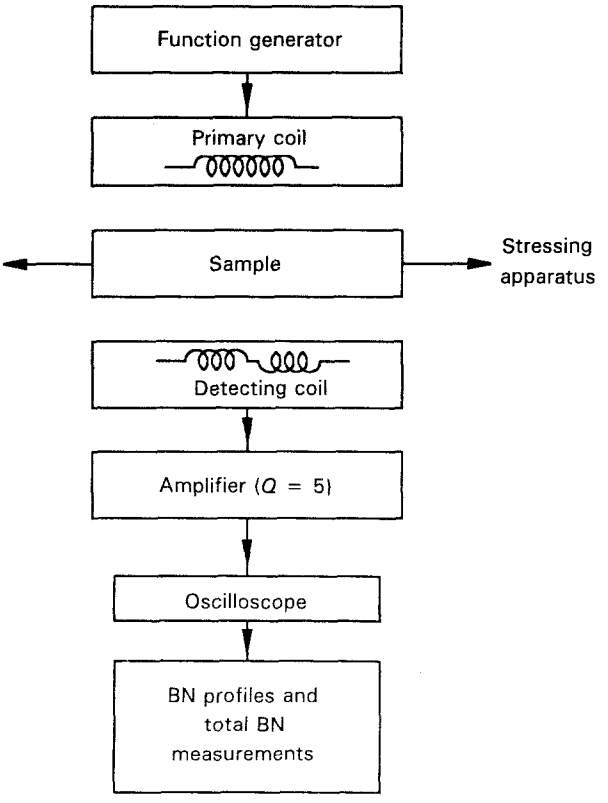

Figure 1 A block diagram of the experimental set-up.

0022–2461

the same number of turns (200) but in opposite directions (the so-called encircling type), and they were located coaxially inside the primary coil generating the magnetic field.

The stressing device consisted of a spring with a spring constant of 1.45×10^3 N m^{-1}. It was used to apply tensile stresses in the elastic range 0–70 MPa to the sample inside the primary coil, in order to measure simultaneously the magnetic properties referred to above. The applied stress was large enough to produce significant changes in the magnetic properties. The fracture tensile stress, measured for the sample independently on an Instron machine, was shown to be 1700 MPa.

A 0.1 Hz triangular waveform magnetic field of $\pm$ 600 A m^{-1} range was generated by a function generator (HP8116A) to saturate the sample in the primary coil. The BN voltage profile, under a constant applied tensile stress, was amplified at a central frequency of 1 kHz using an amplifier (SR530) with a Q-factor of 5, and it was recorded on a digital oscilloscope (LeCroy 9410). The total BN, $(BN)_{tot}$, was obtained by integrating the BN voltage profiles during a half B–H loop.

3. The variation of the initial permeability with stress

The quenched-in stress gave rise to a complex pattern of fine and curved domains on the specimen surface which provided two regions of domains inside the amorphous ribbons: the domain oriented parallel and transverse to the longitudinal ribbon direction, whose volume fractions are designated, respectively, as $v_\parallel$ and $v_\perp$ in the demagnetized state [8]. Since 2605SC has a positive magnetostriction, $v_\perp$ is associated with a transverse anisotropy constant, $K_\perp$, and a compressive stress, σ_c, while $v_\parallel$ is associated with a longitudinal anisotropy constant, $K_\parallel$, and a tensile stress, σ_t.

The dependence of the initial magnetic permeability on the uniaxial applied stress was discussed by Chiriac and Gobotaru [9] by taking into account the magnetization rotation process inside $v_\perp(\sigma)$ and the domain-wall displacement inside $v_\parallel(\sigma)$. Therefore, the initial permeability, $\mu(\sigma)$, under a small alternating current (a.c.) perturbing field can be written as [9]

$$\mu(\sigma) = \mu_0 M_s^2 \left\{ \frac{v_\parallel(\sigma)}{N} + \frac{v_\perp(\sigma)}{N + 2K_\perp(\sigma)} \right\} \quad (1)$$

where μ_0 is the permeability of free space, M_s is the saturation magnetization and N is a proportional coefficient of magnetostatic energy depending on the thermal and mechanical history of the sample, and σ is the applied stress.

The transverse anisotropy constant, $K_\perp(\sigma)$, is given by

$$\begin{aligned} K_\perp(\sigma) &= 3/2\lambda_s(-|\sigma_c| + \sigma) \quad (\sigma < |\sigma_c|) \\ &= 0 \qquad\qquad\qquad\quad (\sigma \geq |\sigma_c|) \end{aligned} \quad (2)$$

where λ_s is the saturation magnetostriction coefficient. The transverse anisotropy constant decreased with the applied tensile stress, and it became zero for $\sigma \geq |\sigma_c|$. As the tensile stress was applied to the sample, $v_\perp(\sigma)$ decreased with the stress level and it exceeded the compressive stress, $\sigma \geq |\sigma_c|$, due to reorientation of the magnetization. As a result, $v_\parallel(\sigma)$ increased at the expense of the transverse volume fraction, and is signified by the increase in $\mu(\sigma)$, which depended on the stress level.

The increase in $\mu(\sigma)$ with the applied tensile stress is shown in Fig. 2. The rapid increase in $\mu(\sigma)$ for small applied stresses, $\sigma < 20$ MPa, arises from decreases in $K_\perp(\sigma)$ and $v_\perp(\sigma)$, and/or increases in $v_\parallel(\sigma)$; See Equation 1. The plateau of $\mu(\sigma)$ for $\sigma > 20$ MPa signifies that the most domains were aligned in the longitudinal ribbon direction; that is, $v_\parallel(\sigma) \approx 1$ and $v_\perp(\sigma) \approx 0$.

4. The characteristics of the BN in relation to domain nucleation/annihilation

The change in the irreversible magnetic flux density is caused by the change of the magnetic moment during the nucleation/annihilation and by the displacement of domain walls [10]. However, the change of the irreversible magnetic flux density due to the displacement of domain walls is negligible in the 2605SC sample, since the domain walls are slightly pinned [9]. Therefore, the major contribution to the irreversible flux change arises from the domain nucleation/annihilation by the domains in $v_\parallel$ rather than the domains in $v_\perp$. These make the dominant contribution to the BN signal because the domain-wall energy in $v_\parallel$ is twice that in $v_\perp$ [11]. Then the irreversible magnetic flux density, B_{irr}, inside $v_\parallel$ can be described by

$$B_{irr} = aN_{n,a}v_\parallel \quad (3)$$

where a is the irreversible magnetic flux density generated when the magnetic moment in the single reversing domain exceeds the domain-wall energy, which embraces the potential barrier for domain nucleation/annihilation. $N_{n,a}$ is the number density of domain walls participating to nucleation/annihilation in $v_\parallel$.

The characteristics of the BN measured by a detecting coil under an applied stress during the sweeping of magnetic field are proportional to the time

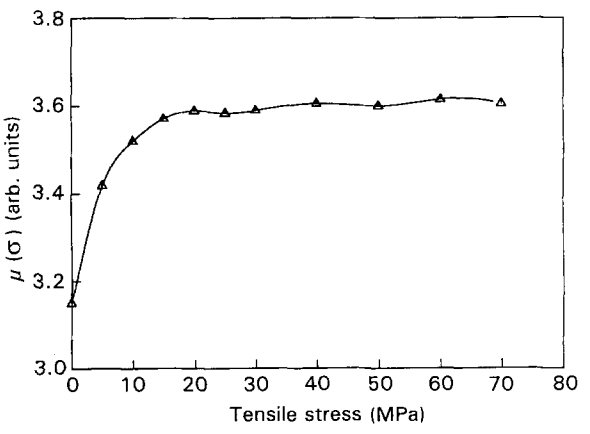

Figure 2 The variation of $\mu(\sigma)$, under a small a.c. perturbing field, with the tensile stress.

derivative of the irreversible magnetic flux, dB_{irr}/dt.

$$BN(H) = c\frac{dB_{irr}}{dt} \tag{4}$$

where c is a dimensional constant converting to the voltage signal which varies with the number of turns and the cross-sectional area of the coil etc.

$$\frac{dB_{irr}}{dt} = a(\sigma)v_{\parallel}(\sigma)\frac{dN_{n,a}(\sigma, H)}{dH}\frac{dH}{dt} \tag{4a}$$

$$c'\,a(\sigma)v_{\parallel}(\sigma)\frac{dN_{n,a}(\sigma, H)}{dH}$$

where dH/dt is a constant for a triangular waveform magnetic field which is denoted by c'. The derivative $dN_{n,a}(\sigma, H)/dH$ represents the distribution of the number density of nucleated/annihilated domains during a half-cycle of magnetization. Therefore, the BN signal in Equation 4 signifies the distribution of nucleation and annihilation of domains during a half B–H loop cycle. Consequently, the total BN, $(BN)_{tot}$, during a half cycle is obtained by integration of the BN profile in Equation 4, as follows

$$(BN)_{tot} = \int_{\text{half cycle}} c\frac{dB_{irr}}{dt}dH \tag{5}$$

$$= c''\,a(\sigma)v_{\parallel}(\sigma)N_{n,a}(\sigma)$$

where c'' is a constant, equal to the product of c and c'. Thus, $(BN)_{tot}$ is proportional to $a(\sigma)N_{n,a}(\sigma)$ and $v_{\parallel}(\sigma)$ during half a hysteresis loop.

5. Results and discussion

The second harmonics under the small applied a.c. magnetic field, $P_2(H)$, are equivalent to the second derivatives of the magnetic induction with respect to the field [12], and the peaks of the second harmonics correspond to the nucleation and annihilation fields H_n and H_a, respectively, measured at 20 Hz with a small a.c. perturbing field, $H_{max} = 20\ A\,m^{-1}$. The variations of the second harmonics with the magnetic field at various tensile stresses are presented in Fig. 3 where the field interval, $\Delta H_{n,a}$ and the height of peaks increase up to about 20 MPa; they remain constant over 20 MPa. Thus, $P_2(H)$ is proportional to $dN_{n,a}(\sigma, H)/dH$ in Equation 4a, which represents the rate of the domain-wall nucleation/annihilation.

The BN profiles for 1 kHz analysing frequency at 0, 10, 20, 40 and 70 MPa are shown in Fig. 4. The prominent single peak of the BN profiles, which is broader than $\Delta H_{n,a}(0)$ under zero stress, is caused by the overlapping of the BN generated during the nucleation and annihilation of the domain walls. The small fluctuating peaks at both sides of the main BN peak may be caused by domain rotation from the saturation magnetization to the local easy axis because of the local compressive stress inside $v_{\perp}(0)$ before the domain nucleation/annihilation takes place. As the stress increased, the single peak of the BN profile under zero stress spilt into two peaks of nucleation and annihilation fields, and the BN profile broadened; and H_n and H_a shifted toward lower and higher applied magnetic fields respectively. The higher nucleation BN peak, compared to the annihilation BN peak, in Fig. 4 is the same as the behaviour observed in 3%SiFe single crystals [4], and in annealed and textured materials [2–3], however, the mechanism has yet to be explained.

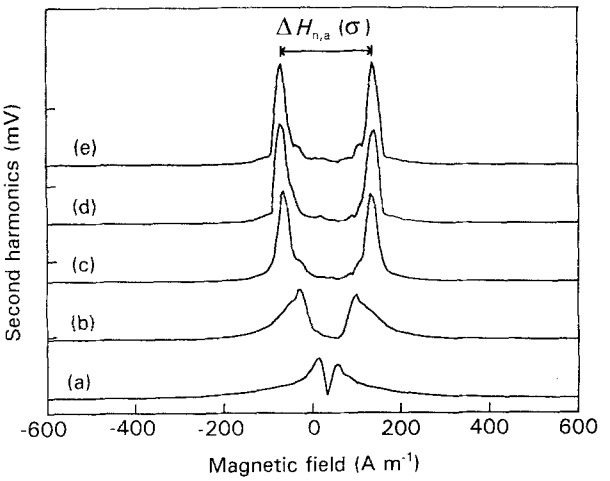

Figure 3 The variation of the second-harmonics curves with the magnetic field under applied tensile stresses of: (a) 0 MPa, (b) 10 MPa, (c) 20 MPa, (d) 40 MPa, and (e) 70 MPa.

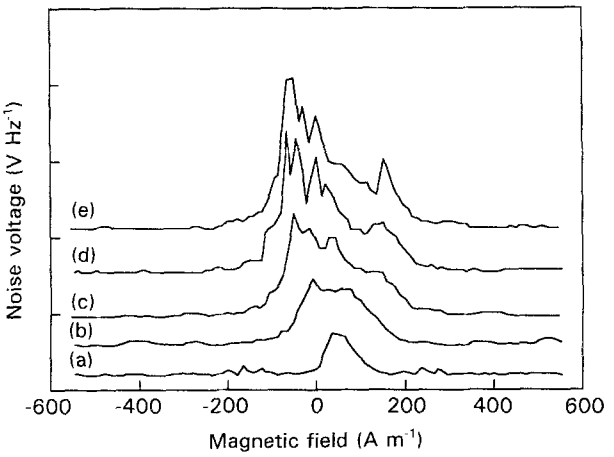

Figure 4 The variation of BN profiles (at a 1 kHz analysing frequency) with magnetic field for applied tensile stresses of: (a) 0 MPa, (b) 10 MPa, (c) 20 MPa, (d) 40 MPa, and (e) 70 MPa.

A plot of semi-logarithmic $(BN)_{tot}$ (normalized by the zero stress) versus the tensile stress is shown in Fig. 5. $(BN)_{tot}$ increased rapidly with the applied tensile stress for $\sigma < 20$ MPa (stage I), and then it slowly increased for $\sigma > 20$ MPa (stage II). The two straight lines with different slopes were obtained by least square fitting and they divided into two regions at 20 MPa. The increase of the normalized $(BN)_{tot}$ can be described by the product of $a(\sigma)$, $N_{n,a}(\sigma)$ and $v_{\parallel}(\sigma)$ in Equation 5, although the exact nature of the increase in each of these parameters is unknown. However, Fig. 5 suggests that $(BN)_{tot}$ increases exponentially with tensile

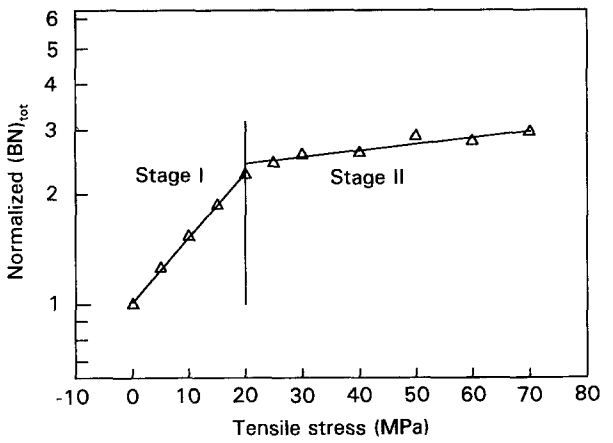

Figure 5 The total BN normalized by the zero stress plotted against the tensile stress, at an analysing frequency of 1 kHz.

stress since

$$(BN)_{tot} = c'\, a(\sigma)\, v_{\parallel}(\sigma)\, N_{n,a}(\sigma) \propto e^{\beta\sigma} \tag{6}$$

where β is a constant representing the two slopes in Fig. 5 where

$$\beta_1 = 1.761 \times 10^{-2} \quad \text{(in stage I)}$$
$$\beta_2 = 1.758 \times 10^{-3} \quad \text{(in stage II)} \tag{7}$$

In fact, $\mu(\sigma)$ in Fig. 2 suggests that $v_{\parallel}(\sigma)$ increases in the ribbon direction for $\sigma < 20$ MPa and $v_{\parallel}(\sigma) \approx 1$ for $\sigma > 20$ MPa with applied tensile stress. The domains may have a complex pattern due to the interaction of the magnetization inside $v_{\parallel}$ and $v_{\perp}$ for $\sigma < 20$ MPa, while simple domains mostly oriented along the ribbon axis prevail for $\sigma > 20$ MPa.

β_2 is very small for stage II in comparison with β_1 in stage I, and thus the series expansion of Equation 6 yields

$$(BN)_{tot} \propto \beta_2 \sigma \tag{8}$$

We consider that the change of the irreversible magnetic flux by domain nucleation/annihilation in stage II is proportional to the single-domain-wall energy, $\gamma(\sigma)$ [13], since

$$a(\sigma) \propto \gamma(\sigma) \propto (K_{\parallel})^{1/2} \tag{9}$$

where the uniaxial anisotropy constant to the ribbon direction, $K_{\parallel}(\sigma)$, inside $v_{\parallel}(\sigma)$ increases linearly with applied tensile stress since

$$K_{\parallel}(\sigma) = 3/2\lambda_s(\sigma_t + \sigma) \tag{10}$$

Thus, $a(\sigma)$ is proportional to the square root of the applied tensile stress, $a(\sigma) \propto \sigma^{1/2}$, and Equation 6 can be rewritten as

$$(BN)_{tot} \propto \sigma^{1/2} N_{n,a}(\sigma) \propto \beta_2 \sigma \tag{11}$$

The average domain width has been shown to decrease with the applied tensile stress in 2605SC (annealed for 2 h at 345 °C [14]) and in grain-oriented 3% SiFe [15], which suggests that the number density of domain walls, $N_{n,a}(\sigma)$, increases with the applied tensile stress. The linear relationship between the applied tensile stress and $(BN)_{tot}$ in stage II leads us to conclude that $N_{n,a}(\sigma)$ is proportional to $\sigma^{1/2}$.

6. Conclusion

The stress dependence of the BN profile and of $(BN)_{tot}$ during a half B–H loop was investigated in a $Fe_{81}B_{13.5}Si_{3.5}C_2$ amorphous ribbon for the as-quenched state. The variation of the initial permeability with the tensile stress indicates that the volume fraction of longitudinal domains along the stress direction increased up to a stress of 20 MPa and then it remained constant at a value with further stressing, $v_{\parallel}(\sigma) \approx 1$. The variation of the second harmonics during the magnetization process under various stresses suggests that the peaks on the BN profiles can be attributed to domain nucleation/annihilation. The two stages of variation of $(BN)_{tot}$, during a half B–H loop, with the tensile stress, transient at 20 MPa, can be described by the exponential relationship $(BN)_{tot} \propto e^{\beta\sigma}$, where there are two different slopes $\beta_1 = 1.761 \times 10^{-2}$ and $\beta_2 = 1.758 \times 10^{-3}$ for stages I and II, respectively. The first stage increment of $(BN)_{tot}$ with the tensile stress is related to the increase of the domain volume fraction parallel to the tensile-stress direction and to the interaction of the magnetization inside both the parallel and transverse domain volumes; however, the second stage can be attributed to the increment in the number of parallel domains and to the potential barrier for domain nucleation/annihilation with tensile stress. The linear increment of $(BN)_{tot}$ in stage II implies that the number of domains involved in the domain nucleation/annihilation is proportional to the square root of the tensile stress, $N_{n,a}(\sigma) \propto \sigma^{1/2}$. The results suggest that BN is more sensitive to the applied tensile stress than to the macroscopic magnetic properties such as the initial permeability or the second harmonics.

Acknowledgements

The authors are grateful to the Korea Advanced Institute of Science and Technology for its financial support in the course of this investigation.

References

1. D. G. HWANG and H. C. KIM, *J. Phys. D.* **21** (1988) 1807.
2. H. C. KIM, K. H. LEE, C. G. KIM and D. G. HWANG, *J. Appl. Phys.* **72** (1992) 3626.
3. G. BERTOTTI, F. FIORILLO and M. P. SASSI, *J. Magn. Magn. Mater.* **23** (1981) 136.
4. G. BERTOTTI, F. FIORILLO and A. M. RIETTO, *IEEE Trans. Magn.* **20** (1984) 1481.
5. C. JAGADISH, L. CLAPHAM and D. L. ATHERTON, *ibid.* **26** (1990) 1160.
6. *Idem, NDT Int.* **22** (1989) 297.
7. A. MITRA and M. VÁZQUEZ, *J. Magn. Magn. Mater.* **87** (1990) 130.
8. M. VÁZQUEZ, W. FERNENGEL and H. KRONMÜLLER, *Phys. Status solidi* (a) **80** (1983) 195.

9. H. CHIRIAC and I. GOBOTARU, *J. Magn. Magn. Mater.* **124** (1993) 277.
10. J. KAMEDA and R. RANJAN, *Acta Metall.* **35** (1987) 1515.
11. R. RAUTIOAHO and P. KARJALINEN, *J. Magn. Magn. Mater.* **61** (1986) 183.
12. A. GARCÍA-ARRIBAS and J. M. BARANDIARÁN, *J. Appl. Phys.* **71** (1992) 3047.
13. B. D. CULLITY "Introduction to magnetic materials" (Addison-Wesley, New York, 1972) p. 287.
14. J. D. LIVINGSTON and W. G. MORRIS, *IEEE Trans. Magn.* **17** (1981) 2624.
15. H. PFÜFZNER, *J. Appl. Phys.* **52** (1981) 3708.

Received 9 November
and accepted 21 December 1993